Numerical Simulation of a Textured and Untextured Photovoltaic Solar Cell: Comparative study

K.Salim, M.N.Amroun, K.Sahraoui, W.Azzaoui

Materials Development and Characterization Laboratory, Department of Electronics, Djillali Liabes University, BP89, Sidi Bel Abbés 22000, Algeria

*Corresponding author; Email: Karim22000@hotmail.com

Article Info

Article history:

Received 26 April, 2021
Revised 19 May, 2021
Accepted 03 June, 2021

Keywords:

Textured silicon
Modelization
Simulation
Solar cell
Photovoltaic

ABSTRACT

Increasing the efficiency of solar cells relies on the surface of the solar cell. In this work, we simulated a textured silicon solar cell. This simulation allowed us to predict the values of the surface parameters such as the angle and depth between the pyramids for an optimal photovoltaic conversion where we found the Icc: 1.783 (A) and Vco: 0.551 (V) with a cell efficiency of about 13.56%. On the other hand, we performed another simulation of a non-textured solar cell to compare our values and found Icc: 1.623 (A) and Vco: 0.556 (V) with an efficiency of about 12.76%.

I. Introduction

Solar energy is the most promising and powerful of the renewable energy sources [1]. Photovoltaic electricity is produced by converting sunlight directly into electricity using photovoltaic cells [2].

Silicon texturing is used to decrease the reflectivity of the surface of the photovoltaic cell [3-4]. This operation aims to develop a micrometric relief on the surface, generally pyramidal in shape. A ray arriving at normal incidence (in relation to the plane of the cell) on the pyramid will be reflected on the face of an adjacent pyramid, this double reflection on the pyramids decreases the total reflection coefficient. Texturing of the surface results in greater trapping of light entering the cell [5-6].

To evaluate the impact of texturing solar cells on cell performance, textured and non-textured photovoltaic cells were modeled and then simulated. Indeed, the simulation of textured cells allows the prediction of the values of the surface parameters for the control of the phenomenon of light trapping (the angle and depth between the pyramids) as well as an evaluation of the surface or interface passivation (SiO_2/ Si) to reduce the rate of recombination, this facilitates lead to a practical realization.

This numerical simulation was carried out from a mathematical model adapted to the textured solar cell. To reduce the degree of complexity of calculations, we chose the model of the electric circuit equivalent to a diode. Nonlinear equations deduced from these models were solved by an iterative method (Newton Raphson method) and through calculation software (Matlab). We have based on two main parameters of a texture (pyramids), these are the height (depth) of the pyramid h, and the density (number) Npyr of the pyramids per unit area.

II. Numerical modeling of a solar cell

For this work, a moderate complexity model was used, the dependence on the diode current and the reverse saturation current is included. The series resistor was included, but not the shunt resistor. A simple shunt diode (Fig. 1) was used to achieve the best shape of the I (V) curve.

This model assumes that the dark current of a solar cell can be described by a single exponential dependence e ’and by a diode quality factor (see equation 2). The values of the equation parameters must be determined to reproduce the I (V) curve. This requires five-variable equations containing five unknowns which will be solved simultaneously to obtain the parameter values. There are three key points on the IV curve of a photovoltaic cell.

The operation of a photovoltaic module is described by the "standard" model with one diode (Fig. 1), established by Shokley for a single PV cell, is generalized to a PV module considering it as a set of identical cells connected in series or in parallel.

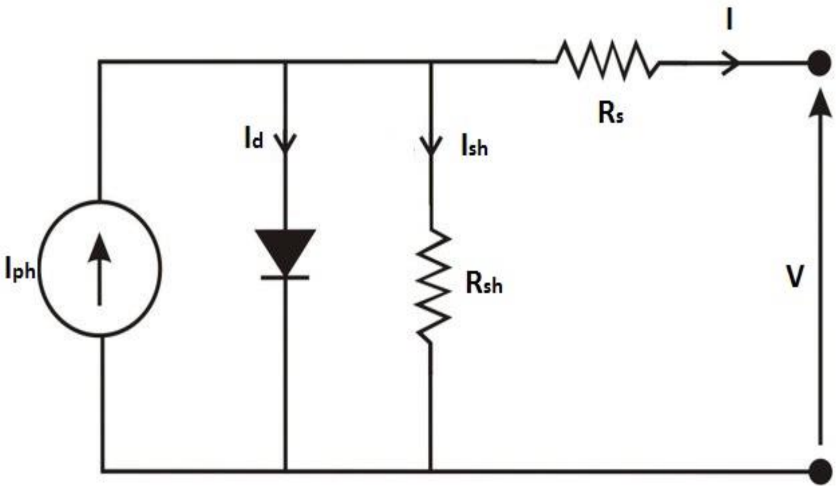

Figure 1. Equivalent diagram of a model PV cell with one diode.

The current supplied by the cell is given by the following relation [7-9]:

$$I = -I_{ph} + \frac{V - R_s I}{R_{sh}} + I_s \left[\exp\left\{ \frac{q(V - R_{sI}}{AKT} \right\} - 1 \right] \tag{1}$$

With :

I_{ph}: Photocurrent,
I_{sh}: Current of the shunt resistor,
I_s: Current of saturation,
R_s: Series resistance Ω,
R_{sh}: Shunt resistance Ω,
q: Charge of the electron = 1,602. 10^{-19} Coulomb,
K: Boltzmann constant (J / K) =1,38.10^{-23} (J/K),
T: Absolute temperature of the Kelvin cell (K).
A: Coefficient of ideality of the dimensionless diode 1<A<5.

From the equivalent circuit of figure (1), we can write:

$$I_{ph} = I_d + I + IR_{sh} \tag{2}$$

The current flowing through the resistor Rsh is given by:

$$I_{Rsh} = \frac{V + IR_S}{R_{sh}} \tag{3}$$

The current in the diode is given by:

$$I_d = I_s \times \left[e^{\frac{q\times(V+R_S I)}{AKT}} - 1 \right] \tag{4}$$

With Is: saturation current of the diode given by:

$$I_s = \frac{I_{cc}}{\exp(qV_{co} / AkT)} \tag{5}$$

So the expression of the characteristic I (V) is [4-5]:

$$I = I_{ph} - I_s \left[\exp\left\{ \frac{q(V - R_s I)}{AKT} \right\} - 1 \right] - \frac{V - R_s I}{R_{sh}} \tag{6}$$

After eqaution (6) obtained; a numerical solution can be obtained using Newton Raphson's algorithm or other algorithms that solve systems of nonlinear equations.

II.a The Newton Raphson Method:

In numerical analysis, the Newton-Raphson method in its simplest application, an efficient algorithm for numerically finding a precise approximation of a zero (or root) of a real function of a real variable. This method owes its name to the English mathematicians Isaac Newton (1643-1727) and Joseph Raphson (possibly 1648-1715), who were the first to describe it for the search for the zeros of a polynomial equation [10-12].

A set of nonlinear matrix-shaped equations is given by:

$$f(x) = \begin{bmatrix} f_1(x) \\ f_2(x) \\ \vdots \\ f_N(x) \end{bmatrix} = y \tag{7}$$

where y and x are n vectors and f (x) is an N vector of functions. The goal is to find x given y and f (x). The equation (7) is rewritten as:

$$0 = y - f(x) \tag{8}$$

and adding Dx to both sides of equation (8), where D is a square N.N,

$$Dx = Dx + y - f(x) \tag{9}$$

And if we multiply by D^{-1} we get:

$$x = x + D^{-1}[y - f(x)] \tag{10}$$

The Newton-Raphson method specifies the matrix D on the basis of Taylor expansion, of x around a point x0.

$$y = f(x_0) + \frac{df}{dx}\Big|_{x=x_0}(x - x_0) \tag{11}$$

The value x0 is replaced by the old value x (i) x and the new value of x (i + 1):

$$x(i+1) = x(i) + J^{-1}(i)\{y - f(x(x(i))\} \tag{12}$$

and the Jacobian matrix J is given for each iteration:

$$J(i) = \frac{df}{dx}\Big|_{x=x(i)} = \begin{bmatrix} \frac{\partial f_1}{\partial x_1} \frac{\partial f_2}{\partial x_2} \cdots \frac{\partial f_1}{\partial f_N} \\ \frac{\partial f_2}{\partial x_1} \frac{\partial f_2}{\partial x_2} \cdots \frac{\partial f_2}{\partial x_N} \\ \\ \frac{\partial f_N}{\partial x_1} \frac{\partial f_N}{\partial x_2} \cdots \frac{\partial f_N}{\partial x_N} \end{bmatrix} \tag{13}$$

So according to our equations (1.2.3.4.5.6) the Jacobian matrices will be as follows:

For Jacobian (1) :

$$\begin{aligned} &J(1.1) = 1 \\ &J(1.2) = -\exp\left(\frac{qV_{co}}{AkT}\right) + 1 \\ &J(1.3) = -\frac{qI_s V_{co} \exp\left(\frac{qV_{co}}{AkT}\right)}{A^2 kT} \\ &J(1.4) = 0 \\ &J(1.5) = -\frac{V_{co}}{R_{sh}^2} \end{aligned} \tag{14}$$

For Jacobian (2) :

$$J(2.1) = 1 \quad (15)$$

$$J(2.2) = -\exp\left[\frac{qI_{cc}R_s}{AkT}\right] + 1$$

$$J(2.3) = \frac{qI_sI_{cc}R_s \exp\left[\frac{qI_{sc}R_s}{AkT}\right]}{A^2kT}$$

$$J(2.4) = \frac{qI_sI_{cc} \exp\left[\frac{qI_{cc}R_s}{AkT}\right]}{AkT} - \frac{I_{cc}}{R_{sh}}$$

$$J(2.5) = \frac{I_{cc}}{R_{sh}^2}$$

For Jacobian (3) :

$$J(3.1) = 0 \quad (16)$$

$$J(3.2) = \frac{q(1 - \frac{R_s}{R_{sh}})\exp(\frac{qV_{co}}{AkT})}{AkT}$$

$$j(3.3) = \frac{qI_s(R_s - R_{sh})\exp(\frac{qV_{co}}{AkT})(AkT + qV_{co})}{A^3k^2T^2R_{sh}}$$

$$J(3.4) = \frac{qI_s(R_s - R_{sh})\exp(\frac{qV_{co}}{AkT})}{AkTR_{sh}} + \frac{1}{R_{sh}.R_s}$$

$$J(3.5) = \frac{1 - \frac{R_s}{R_{sh}}}{R_{sh}^2}$$

For Jacobian (4) :

$$J(4.1) = 0 \quad (17)$$

$$J(4.2) = -\frac{q(1 - \frac{R_s}{R_{sh}})\exp(\frac{qI_{cc}R_s}{Akt})}{AkT}$$

$$J(4.3) = \frac{qI_s(R_{sh} - R_s)\exp(\frac{qI_{cc}R_s}{AkT})(AkT + qI_{cc}R_s)}{A^3k^2T^2R_{sh}}$$

$$J(4.4) = \frac{qI_s(R_{sh} - R_s)\exp(\frac{qI_{cc}R_s}{AkT})}{AkTR_{sh}} - \frac{q^2I_s(1 - \frac{R_s}{R_{sh}})I_{sc}\exp\left[\frac{qI_{cc}R_s}{AkT}\right]}{A^2k^2T^2} + \frac{1}{R_{sh}R_s}$$

$$J(4.5) = \frac{R_{sh} - R_s}{R_{sh}^2R_s}$$

For Jacobian (5) :

$$J(5.1) = 0 \tag{18}$$

$$J(5.2) = -\frac{q(1-\frac{I_{pm}R_s}{V_{pm}})\exp(\frac{q(V_{pm}+I_{pm}R_s)}{AkT})}{AkT}$$

$$J(5.3) = \frac{(V_{pm}-I_{pm})\left[AkT+q(V_{pm}+I_{pm}R_s)\right]qI_s\exp(\frac{q(V_{pm}+I_{pm}R_s)}{Akt}}{V_{pm}A^3k^2T^2}$$

$$J(5.4) = \frac{qI_sI_{pm}\exp(\frac{q(V_{pm}+I_{pm}R_s)}{AkT})}{V_{pm}AkT}\ \frac{q^2I_s(1-\frac{I_{pm}R_s}{V_{pm}})I_{pm}\exp(\frac{q(V_{pm}+I_{pm}R_s)}{AkT})}{A^2k^2T^2}+\frac{I_{pm}}{R_{sh}.V_{pm}}$$

$$J(5.5) = \frac{1-\frac{I_{pm}R_s}{V_{pm}}}{R_{sh}^2}$$

The Jacobian is used to facilitate finding a solution for our nonlinear equation (6) using MATLAB software. All constants in the equations can be determined using data from PV panel manufacturers.

III. Numerical simulation of a textured solar cell

III.1 Principle of simulation:

In this simulation we have based on two main parameters of a texture (pyramids), these are the height (depth) of the pyramid h, and the density (number) Npyr of the pyramids per unit area.

III.2 Simulation of the textured surface:

The diagram shows (Fig.2) all the dimensions and parameters of a pyramid (several pyramids in each row).

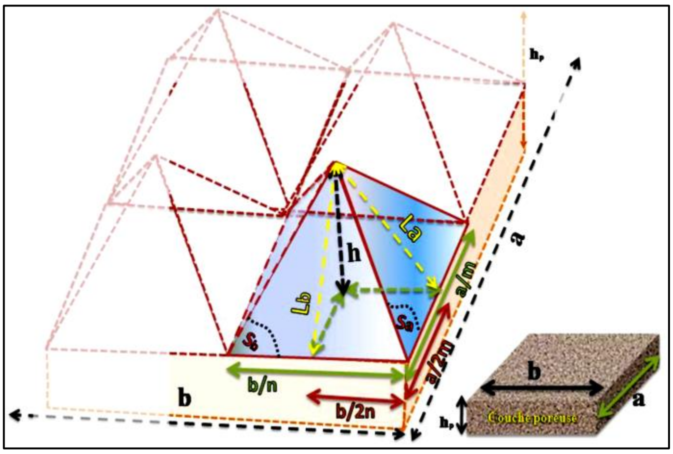

Figure 2. Diagram shows the notations of different dimensions of a pyramid.

With S_a and S_b, are the surface of triangle side "a" and side "b", respectively:

The number of pyramids $N_{pyr} = m \times n$ then the total area Stot is:

$$\left\{ \begin{array}{l} S_a = \frac{a}{2m} \times L_a \\ L_a = \sqrt{h^2 + \left(\frac{b}{2n}\right)^2} \end{array} \right\} \Rightarrow S_a = \frac{a}{2m} \times \sqrt{h^2 + \left(\frac{b}{2n}\right)^2} \tag{19}$$

S_{pyr} is the complete area of a pyramid, then:

$$S_{pyr} = 2(S_a + S_b) = \frac{a}{m}.\sqrt{h^2 + \left(\frac{b}{2n}\right)^2} + \frac{b}{n}.\sqrt{h^2 + \left(\frac{a}{2m}\right)^2} \tag{20}$$

The number of pyramids $N_{pyr} = m \times n$ then the total area Stot is:

$$S_{tit} = N_{pyr} \times S_{pyr} \Rightarrow S_{tot} = m.n\left(\frac{a}{m}.\sqrt{h^2 + \left(\frac{b}{2n}\right)^2} + \frac{a}{n}.\sqrt{h^2 + \left(\frac{a}{2m}\right)^2}\right) \tag{21}$$

To facilitate the calculation we do: $a = b, m = n = \sqrt{N_{pyr}}$, we get the following relation:

$$S_{tot} = N_{pyr}.\left(\frac{2a}{\sqrt{N_{pyr}}.}.\sqrt{h^2 + \left(\frac{a}{2\sqrt{N_{pyr}}}\right)^2}\right) \tag{22}$$

$$\Rightarrow S_{tot} = 2.a\sqrt{N_{pyr}}.\sqrt{h^2 + \left(\frac{a}{2\sqrt{N_{pyr}}}\right)^2}$$

$$\Rightarrow S_{tit} = 2.a\sqrt{N_{pyr}} \times \frac{a}{2.\sqrt{N_{pyr}}}\sqrt{\left(\frac{2.h.\sqrt{N_{pyr}}}{a}\right)^2 + 1}$$

$$\Rightarrow S_{tot} = a^2.\sqrt{\left(\frac{2.h.\sqrt{N_{pyr}}}{a}\right)^2 + 1}$$

In general the surface of the cell is as follows:

$$S_{tot} = \left\{ \begin{array}{l} a^2 \Rightarrow; h = 0, N_{pyr} = 1 \Rightarrow area(plane \Rightarrow untextured) \\ a^{2.}.\sqrt{\left(\frac{2.h.N_{pyr}}{a}\right)^2 + 1} \Rightarrow h \neq 0, N_{pyr} \rangle\rangle 1 \Rightarrow area(textured) \end{array} \right\} \tag{23}$$

IV. Results

All of the constants in the all obtained equations can be determined using manufacturer data from 36-cell solar panel, and from the I(V) curves. The ENIE Solar 75 (W) module will be used to illustrate and verify the simulation model we used.

Table 1: electrical characteristic of the ENIE Solar photovoltaic module

The parameters	Value
Maximum Power (P_{max})	75 W +/- 10%
Voltage at Pmax (V_{max})	17.3 W
Current at Pmax (I_{max})	4.05 A
Voltage at open circuit (V_{co})	21.6 V
Current of short-circuit (I_{cc})	4.67 A

Parameters of a photovoltaic solar cell of the ENIE Solar 75 (W) module were characterized in laboratory of development and characterization of materials (LECM), University of Djilali Liabes Sidi bel-abbès. Algeria.

Table 2 : Simulated solar cell parameters

The paramètres	Symbol	Value
Area	S	50 cm²
The reflection coefficient	R	0 % ~ 30 %
number of pyramids	N_{pyr}	0 ~ 3000
the height (depth) of the pyramid	h	0 ~ 6 *um*
flux power per unit area	P	2 ,51.10^{-3} w /m²

With the MATLAB 2011 program that we used for the simulation of the characteristics of our photovoltaic generator), we will simulate a mathematical model of the photovoltaic solar cell which has been characterized in our laboratory (LECM), and we will study it in two cases (with the variation of the height, number of pyramids and the reflectance).

The 1st case: when it is textured: h and N pyr greater than 0 and 1 (Fig. 3)

The 2nd case: when it is not textured, ie: h = 0 and Npyr = 1 (Fig. 5)

IV.1. Solar cell with texturing with (h= 5 um; R= 10 %; N_{pyr} = 3000):

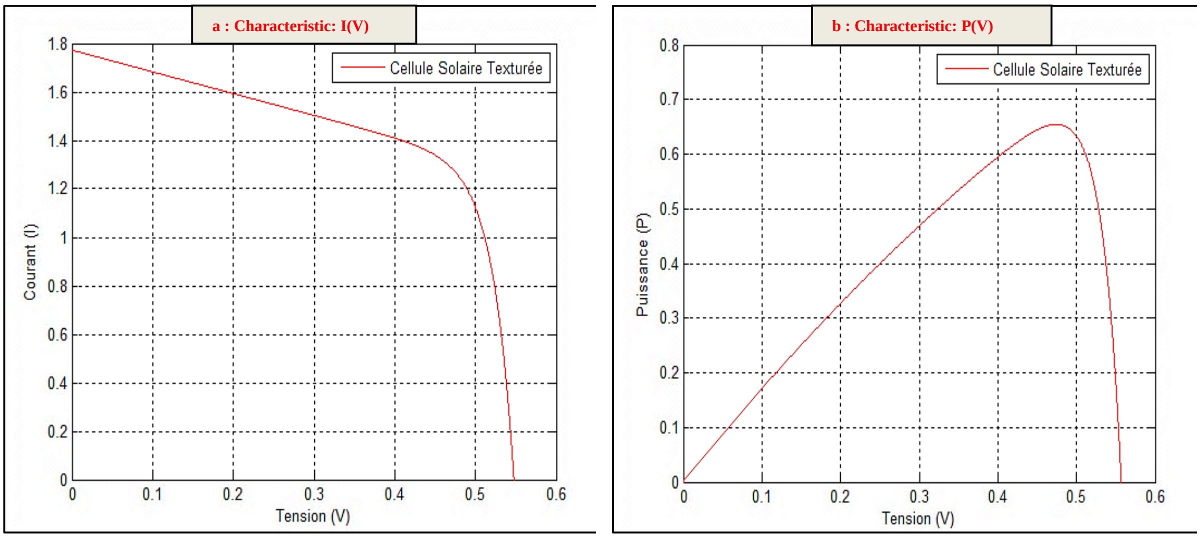

Figure 3. Characteristic a: I(V), b: P(V) of the solar cell with texturing.

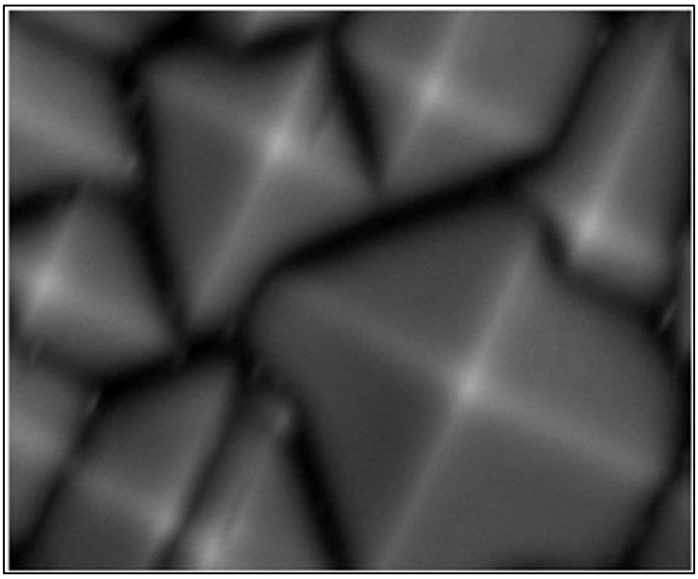

Figure 4. Image of the surface of a textured solar cell (carried out at the LECM laboratory).

Table 3: electrical characteristics of the solar cell with texturing

Current of short circuit	I_{CC}	= 1.783 (A)
Power Max	P_M	= 0.679 (W)
Voltage of open circuit	V_{CO}	= 0.551 (V)
Form factor	*FF*	= 0.712
Efficiency	η	= 13.56 %

IV.2. Solar cell without texturing with (h= 0 ; R= 25 % ; N_{pyr} = 1) :

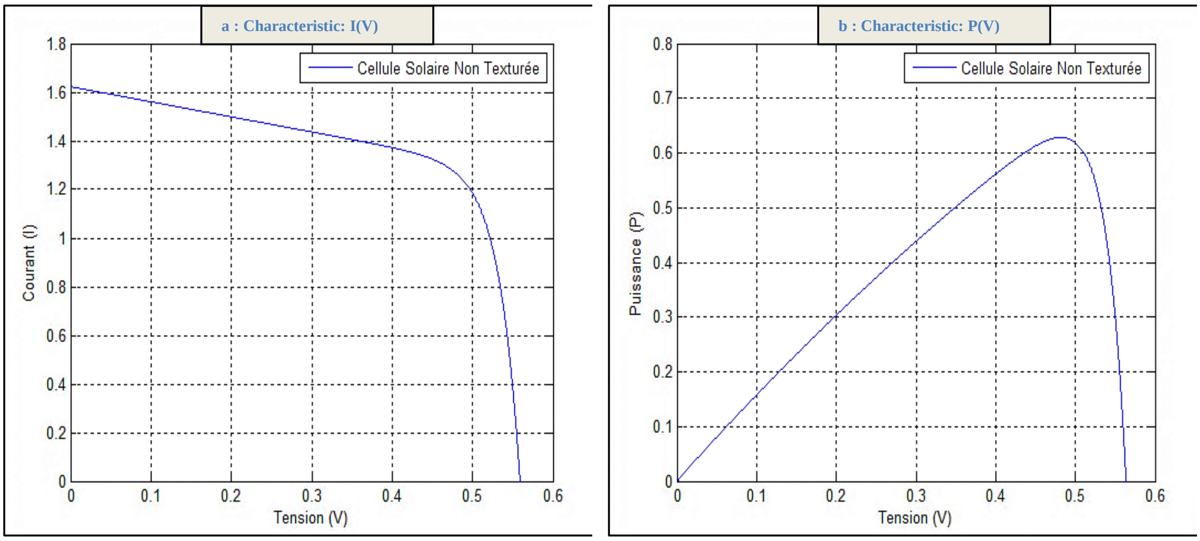

Figure 5. Characteristic a: I(V), b: P(V) of the solar cell without texturing.

Table 4: electrical characteristics of solar cell without texturing

Current of short circuit	I_{CC}	= 1.623 (A)
Power Max	P_M	= 0.638 (W)
Voltage of open circuit	V_{CO}	= 0.556 (V)
Form factor	*FF*	= 0.703
Efficiency	η	= 12.76 %

From the results above we conclude that the pyramid number and the depth of the texturing pyramids are important parameters for a solar cell and consequently the texturing influences the characteristics of the solar cell and especially the short-circuit current Icc with respect to the voltage Vco, because the Isc takes into account the surface of the solar cell where the modifications have been made.

V. Conclusion

Whatever the structure of a solar cell, an optimisation of its parameters is necessary to have a good efficiency. In this work, we simulated a textured silicon solar cell, the results obtained in this paper present the effectiveness of texturing on the characteristics of the solar cell. The simulation performed in this work allows the experimenter to control the surface parameters of the textured silicon for optimal photovoltaic conversion. The results of this simulation provide an improvement in conversion efficiency from 12.76% to 13.56%. The developed model could be embedded into solar cell simulation tools or adapted to predict optical properties of diverse surface morphologies. Finally we concluded that texturing is an important parameter for a solar cell because the trapping of the light which was obtained by the texturing improves the efficiency of the photovoltaic solar cell.

References

[1] Maatallah Elabbes, Berbaoui Brahim, Modelling and Control of Photovoltaic System using the incremental conductance method for maximum power point tracking, Algerian Journal of Renewable Energy and Sustainable Development 1(2) 2019 191-197, https://doi: 10.46657/ajresd.2019.1.2.

[2] Ahmed Idda , Leila Ayat , Said Bentouba, A Review of Different Techniques for Improving the Performance of Amorphous Silicon based Solar Cells , Algerian Journal of Renewable Energy and Sustainable Development 1(2) 2019: 172-181, https://doi:10.46657/ajresd.2019.1.2.6

[3] Belhadj Mohammed, Modeling of a Photovoltaic collection system, Magister's Memory in Microelectronics - Autonomous Photovoltaic, University Center of Bechar, 2008.

[4] P. Campbell and Green, M. A., Light trapping properties of pyramidally textured surfaces, Journal of Applied Physics, vol. 62, no. 1, p. 243, 1987. http://dx.doi.org/10.1063/1.339189.

[5] Baghdadi Faiza, Modeling and Simulation of the Performance of a Hybrid Renewable Energy Conversion Installation, Magister's Memory. Specialty: Mechanical Engineering, Mouloud Mammeri Tizi-ouzou University, 2011.

[6] M. M. de Jong, P. J. Sonneveld, J. Baggerman, C. J. M. van Rijn, J. K. Rath, and R. E. I. Schropp, Utilization of geometric light trapping in thin film silicon solar cells: simulations and experiments, Prog. Photovolt: Res. Appl. 22(5), 540–547 (2014), https://doi.org/10.1364/OE.22.0A1422.

[7] Suneel Raju Pendem, Suresh Mikkili Modeling, simulation and performance analysis of solar PV array configurations (Series, Series–Parallel and Honey-Comb) to extract maximum power under Partial Shading Conditions Energy Reports 4 (2018) 274–287, https://doi.org/10.1016/j.egyr.2018.03.003.

[8] Rameen AbdelHady, Modeling and simulation of a micro grid-connected solar PV system, Water Science 31 (2017) 1–10, http://dx.doi.org/10.1016/j.wsj.2017.04.001.

[9] AminYahya-Khotbehsara, AliShahhoseini, SolarEnergy 162, (2018) 403-409, https: //doi.org/ 10.1016/j.solener. 2018.01.047

[10] F. Ghani , E.F. Fernandez , F. Almonacid , T.S. O'Donovan, The numerical computation of lumped parameter values using the multi-dimensional Newton-Raphson method for the characterisation of a multi-junction CPV module using the five-parameter approach, Solar Energy 149 (2017) 302–313, http://dx.doi.org/10.1016/j.solener.2017.04.024.

[11] F.Ghania, G.Rosengarten, M.Duke, J.K.Carson, The numerical calculation of single-diode solar-cell modelling parameters, Renewable Energy 72 (2014) 105-112, https://doi.org/10.1016/j.renene.2014. 06.035.

[12] Gwinyai Dzimano, Modeling of Photovoltaic Systems, A Thesis Presented in Partia Ful llment of the Requirements for the Degree Master of Science in the Graduate School of The Ohio State University, The Ohio State University. 2008.